1 **Supporting Information for**

2 **Response of the Aerodyne Aerosol Mass Spectrometer to Inorganic Sulfates and**

3 **Organosulfur Compounds: Applications in Field and Laboratory Measurements**

4 *Yunle Chen[1], Lu Xu[2,3], Tim Humphry[4], Anusha P. S. Hettiyadura[5,6], Jurgita Ovadnevaite[7], Shan Huang[8,9],*

5 *Laurent Poulain[9], Jason C. Schroder[10,11], Pedro Campuzano-Jost[10,11], Jose L. Jimenez[10,11], Hartmut*

6 *Herrmann[9], Colin O'Dowd[7], Elizabeth A. Stone[5], Nga Lee Ng[1,2,*]*

7 [1] School of Earth and Atmospheric Sciences, Georgia Institute of Technology, Atlanta, Georgia 30332,

8 United States

9 [2] School of Chemical and Biomolecular Engineering, Georgia Institute of Technology, Atlanta, Georgia

10 30332, United States

11 [3] Now at Division of Geological and Planetary Sciences, California Institute of Technology, Pasadena,

12 CA 91125, United States

13 [4] Department of Chemistry, Truman State University, Kirksville, Missouri 63501, United States

14 [5] Department of Chemistry, University of Iowa, Iowa City, Iowa 52242, United States

15 [6] Now at Department of Chemistry, Purdue University, West Lafayette, Indiana 47907, United States

16 [7] School of Physics and Centre for Climate and Air Pollution Studies, Ryan Institute, National University

17 of Ireland Galway, Galway H91 TK33, Ireland

18 [8] Now at Institute for Environmental and Climate Research, Jinan University, Guangzhou, Guangdong

19 511443, China

20 [9] Leibniz Institute for Tropospheric Research, Leipzig, Sachsen, 04318, Germany

21   [10] Department of Chemistry, University of Colorado, Boulder, Colorado 80309, United States

22   [11] Cooperative Institute for Research in the Environmental Sciences (CIRES), University of Colorado,

23   Boulder, Colorado 80309, United States

24

25   Number of pages: 24

26   Number of figures: 12

27   Number of tables: 4

S1. Details of Chamber Experiment and Field Measurements

S1.1. Chamber Experiment

Isoprene photooxidation SOA under low-NO condition were generated in the Georgia Tech Environmental Chamber (GTEC) facility. Details of the facility have been described in Boyd et al.[1] and details of the experiment have been described in Tuet et al..[2] Briefly, the experiment was performed at 25 $^{\circ}$C under dry (RH < 5 %) condition. Prior to the experiment, the chamber was flushed with zero air for ~24 h. Seed aerosol was first introduced by atomizing 15 mM AS solution and seed volume concentration was stabilized at ~ 25 $\mu m^3/cm^3$. Aerosol volume concentrations and distributions were measured using a scanning mobility particle sizer (SMPS; TSI) consisting of a differential mobility analyzer (DMA; TSI 3040) and a condensation particle counter (CPC; TSI 3775). Isoprene (99%, Sigma-Aldrich) was injected into a glass bulb and zero air was passed over the solution until it evaporated. The initial concentration of isoprene was 97 ppb. H_2O_2 (50% aqueous solution, Sigma-Aldrich) was then injected as an OH precursor. Once the concentrations of all species stabilized, UV lights were turned on to initiate photooxidation. The photolysis of H_2O_2 yielded an OH concentration on the order of 10^6 molecules/cm^3 under low-NO conditions.

S1.1. Field Measurements

The Centreville measurements were performed in Centreville, Alabama (USA), from 01 June to 15 July 2013 during the Southern Oxidant and Aerosol Study (SOAS) with the GT AMS.[3, 4] The Centreville site is a rural site located in a forested area, with high biogenic emissions, especially isoprene and monoterpenes. Biogenic volatile organic compounds (BVOC)-derived organosulfur species have been identified as an abundant contributor to total OA in the southeastern US,[5, 6] making this location ideal for organosulfur compound measurements.

The Mace Head measurements were performed at the Mace Head Global Atmosphere Watch research station, Ireland, from 12 July 2010 to 9 September 2010 with the Galway AMS.[7] This is a ground site located on the west coast of Ireland and facing westward to the northeast Atlantic, where clean marine air coming onshore can be perturbed by (mostly local) anthropogenic sources. In the summertime high oceanic biological activity results in abundant atmospheric MSA at this site.

The Polarstern measurements were performed on the German research vessel (RV) Polarstern during a cruise from Cape Town, Republic of South Africa to Bremerhaven, Germany, from 20 April to 20 May 2011 with the TROPOS AMS. [8] The cruise took place during the autumn in the Southern hemisphere, when both dimethyl sulphide and MSA concentrations are expected to be relatively low, and spring in the Northern hemisphere, where phytoplankton blooms were often encountered, resulting in high MSA concentrations. This spatial contrast was reflected in the MSA concentration time series.

The Wintertime Investigation of Transport, Emissions, and Reactivity (WINTER) aircraft campaign took place out of the NASA Langley Research Center (Hampton, VA) from February 1 to March 15, 2015 aboard the National Center for Atmospheric Research (NCAR) C-130 aircraft, with the Boulder AMS.[9] One campaign objective was to look at the temporal evolution of power plant plumes under low temperature/stagnant conditions typical of the winter months in the northeastern US.

S2. Uncertainty Analysis for Sulfate Apportionment Method

Recall that ΣHSO_{AS}, $\Sigma HSO_{OS/SS}$, and ΣHSO_{MSA} are calculated by Equation (10) in the main text. Including the error of each term we can get:

$$\begin{bmatrix} \Sigma\mathrm{HSO}_{AS} \pm \delta\Sigma\mathrm{HSO}_{AS} \\ \Sigma\mathrm{HSO}_{OS/SS} \pm \delta\Sigma\mathrm{HSO}_{OS/SS} \\ \Sigma\mathrm{HSO}_{MSA} \pm \delta\Sigma\mathrm{HSO}_{MSA} \end{bmatrix} =$$

$$\begin{bmatrix} (f_{HSO_3} \pm \delta f_{HSO_3})_{AS} & (f_{HSO_3} \pm \delta f_{HSO_3})_{OS/SS} & (f_{HSO_3} \pm \delta f_{HSO_3})_{MSA} \\ (f_{H_2SO_4} \pm \delta f_{H_2SO_4})_{AS} & (f_{H_2SO_4} \pm \delta f_{H_2SO_4})_{OS/SS} & (f_{H_2SO_4} \pm \delta f_{H_2SO_4})_{MSA} \\ 1 & 1 & 1 \end{bmatrix}^{-1} \begin{bmatrix} (\mathrm{HSO}_3 \pm \delta\mathrm{HSO}_3)_{meas} \\ (\mathrm{H}_2\mathrm{SO}_4 \pm \delta\mathrm{H}_2\mathrm{SO}_4)_{meas} \\ (\Sigma\mathrm{HSO} \pm \delta\Sigma\mathrm{HSO})_{meas} \end{bmatrix}$$

(S1)

For laboratory calibration of standard compounds, δf_{HSO_3} and $\delta f_{H_2SO_4}$ of pure standard compounds (AS and MSA) were calculated as the standard deviation during calibration when signals were stable, while δf_{HSO_3} and $\delta f_{H_2SO_4}$ of OS/SS were calculated as the standard deviation of all OS and SS compounds calibrated in this study. For uncertainties in the measured mass concentratin of sulfate fragments, $\delta\Sigma\mathrm{HSO}$ was calculated by error propagation:

$$\delta\Sigma\mathrm{HSO}= \sqrt{(\delta\mathrm{SO}^+)^2 + (\delta\mathrm{SO}_2^+)^2 + (\delta\mathrm{SO}_3^+)^2 + (\delta\mathrm{HSO}_3^+)^2 + (\delta\mathrm{H}_2\mathrm{SO}_4^+)^2} \quad (S2)$$

The uncertainties of apportionment results ($\Sigma\mathrm{HSO}_{AS}$, $\Sigma\mathrm{HSO}_{OS/SS}$, and $\Sigma\mathrm{HSO}_{MSA}$) can be then assessed via Monte Carlo approach. For the scaling factor, $\left(\dfrac{\Sigma\mathrm{HSO}}{\text{total sulfate}} \right)_{standard}$, used to convert $\Sigma\mathrm{HSO}$ signals from above calculations to total sulfate signals, the uncertainty was acquired from the standard calibration. The uncertainties of IE determination (~ 10%), CE determination (~ 30%), and RIE determination (~ 15%) were also encapsulated.[10]

Uncertainties for field measurement data were calculated and shown as error bars in **Figure S7**. 1000 sets of parameters were randomly generated for every point and used as inputs in equation (10). The campaign average "AS sulfate", "OS/SS Sulfate", and "MSA Sulfate" uncertainties are

88   26%, 45%, and 23% for Centreville measurements, 36%, 38%, and 90% for Mace Head

89   measurements, 31%, 86%, and 41% for Polarstern measurements.

90   **S3. UMR Data Analysis**

91   In addition to the HR sulfate mass spectra analysis, we also explored the plausibility of

92   deconvolving sulfate signals for UMR data using signals allocated to sulfate at m/z 48 (SO4_48,

93   counterpart of SO^+), m/z 64 (SO4_64, counterpart of SO_2^+), m/z 80 (SO4_80, counterpart of SO_3^+),

94   m/z 81 (SO4_81, counterpart of HSO_3^+), and m/z 98 (SO4_98, counterpart of $H_2SO_4^+$). The results

95   after normalization are shown in **Figure S9**. For most standard compounds, the results resemble

96   those of HR analysis, and sulfate mass spectra of AS, OS/SS, MSA can still be distinguished by

97   the ion fractions of SO4_81 (f_{81}, counterpart of f_{HSO_3}) and SO4_98 (f_{98}, counterpart of $f_{H_2SO_4}$).

98   Sulfate apportionment was applied to UMR data of laboratory-generated binary mixtures, isoprene

99   photooxidation experiment, and one of the field measurements (Centreville SOAS data). For both

100   binary mixtures (MSA+AS, OS+AS), "MSA sulfate" (or "OS Sulfate") to "AS sulfate" molar ratio

101   calculated by the apportionment method correlates well with MSA (or OS) to AS molar ratio in

102   the particles, with $R^2 = 0.998$ and $R^2 = 0.995$, respectively, while UMR analysis overestimates the

103   ratio by a factor of ~2 (**Figure S10**). For the isoprene photooxidation experiment, "OS sulfate"

104   and "AS sulfate" calculated from UMR data are very similar to HR calculations (**Figure S11**). For

105   Centreville measurements, 77% of the "OS sulfate" calculated from UMR data are negative values

106   (**Figure S12**), indicating the UMR-based sulfate apportionment may not perform as well as HR

107   data in complex ambient conditions, but we can still conclude from the analysis of UMR data that

108   "AS sulfate" is the dominant source for sulfate signals in AMS at Centreville.

109

110
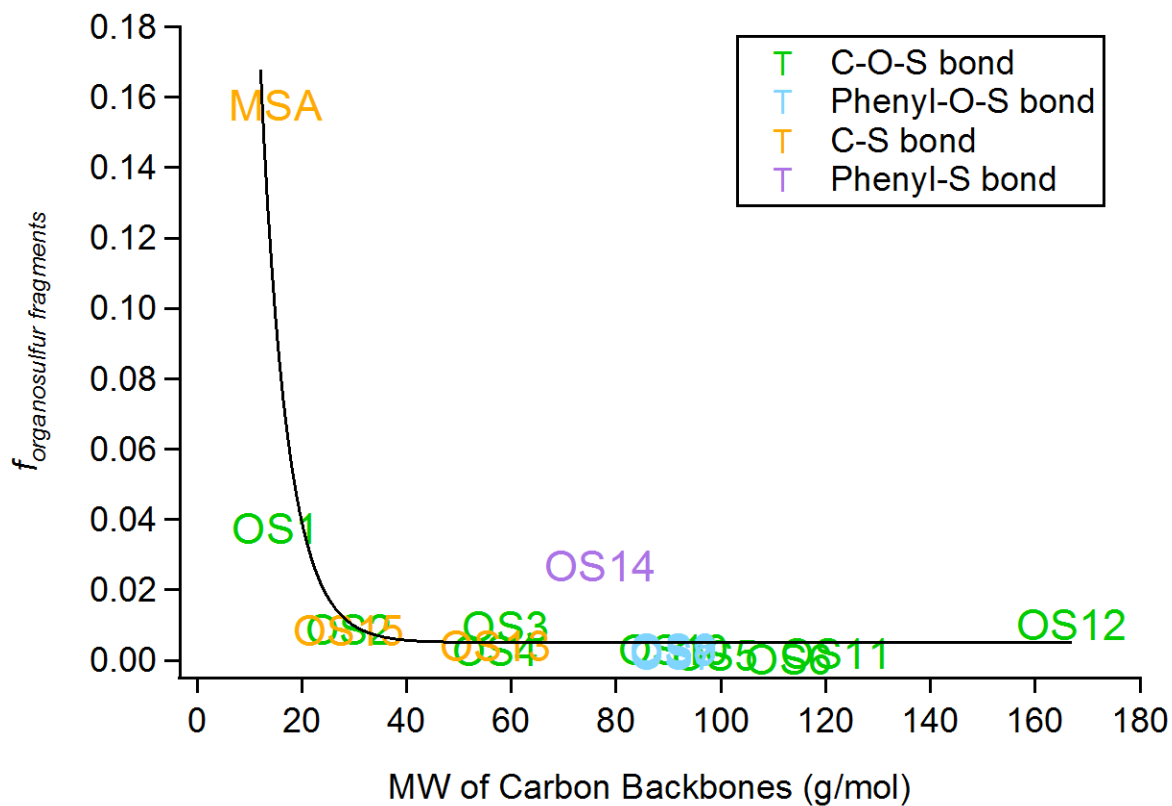
Figure S1 Fractions of organosulfur fragments produced by standard organosulfur compounds in

the AMS as a function of the molecular weight of carbon backbones. The data points are colored
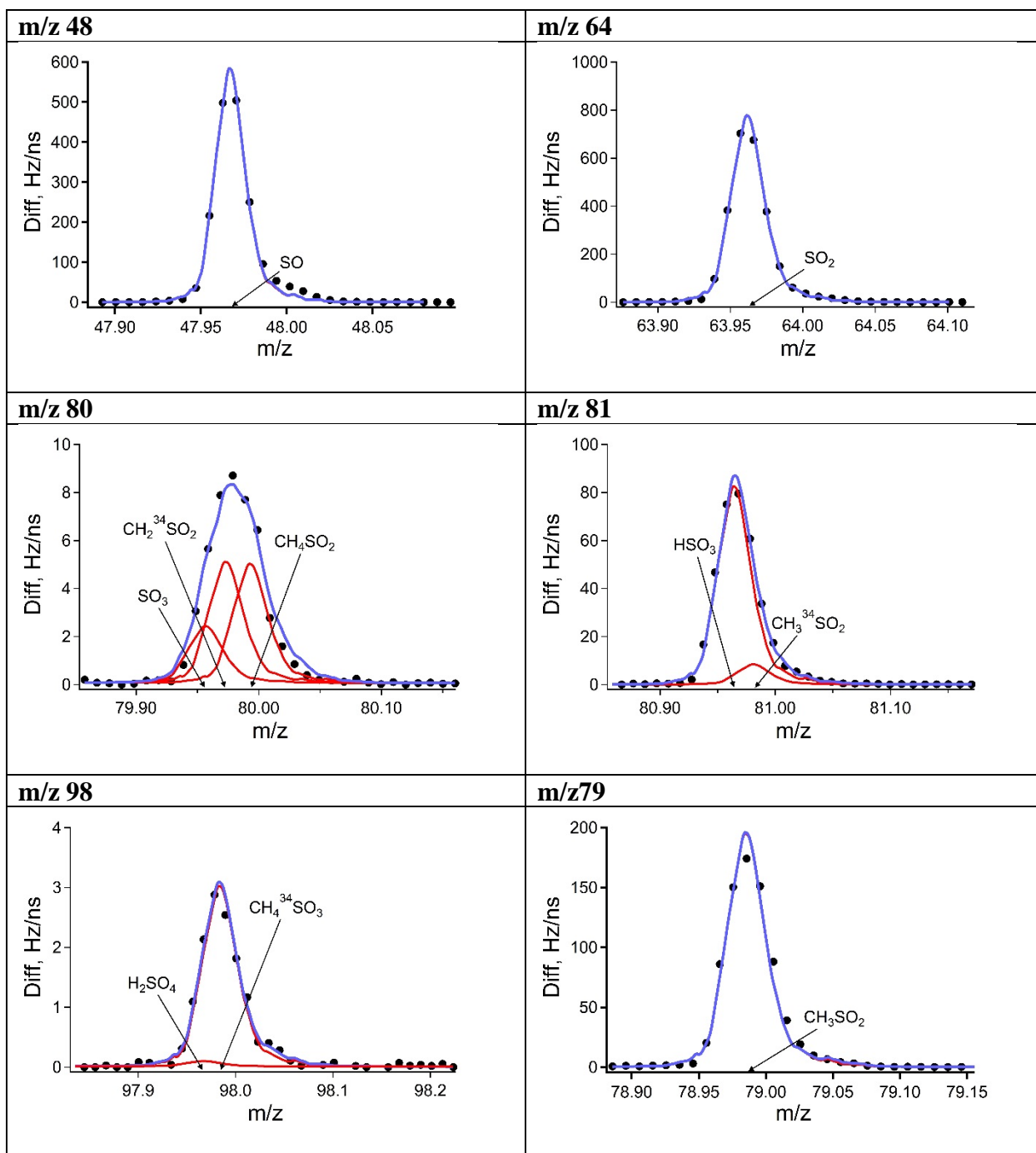
by their carbon backbone structures and bonding types.

114
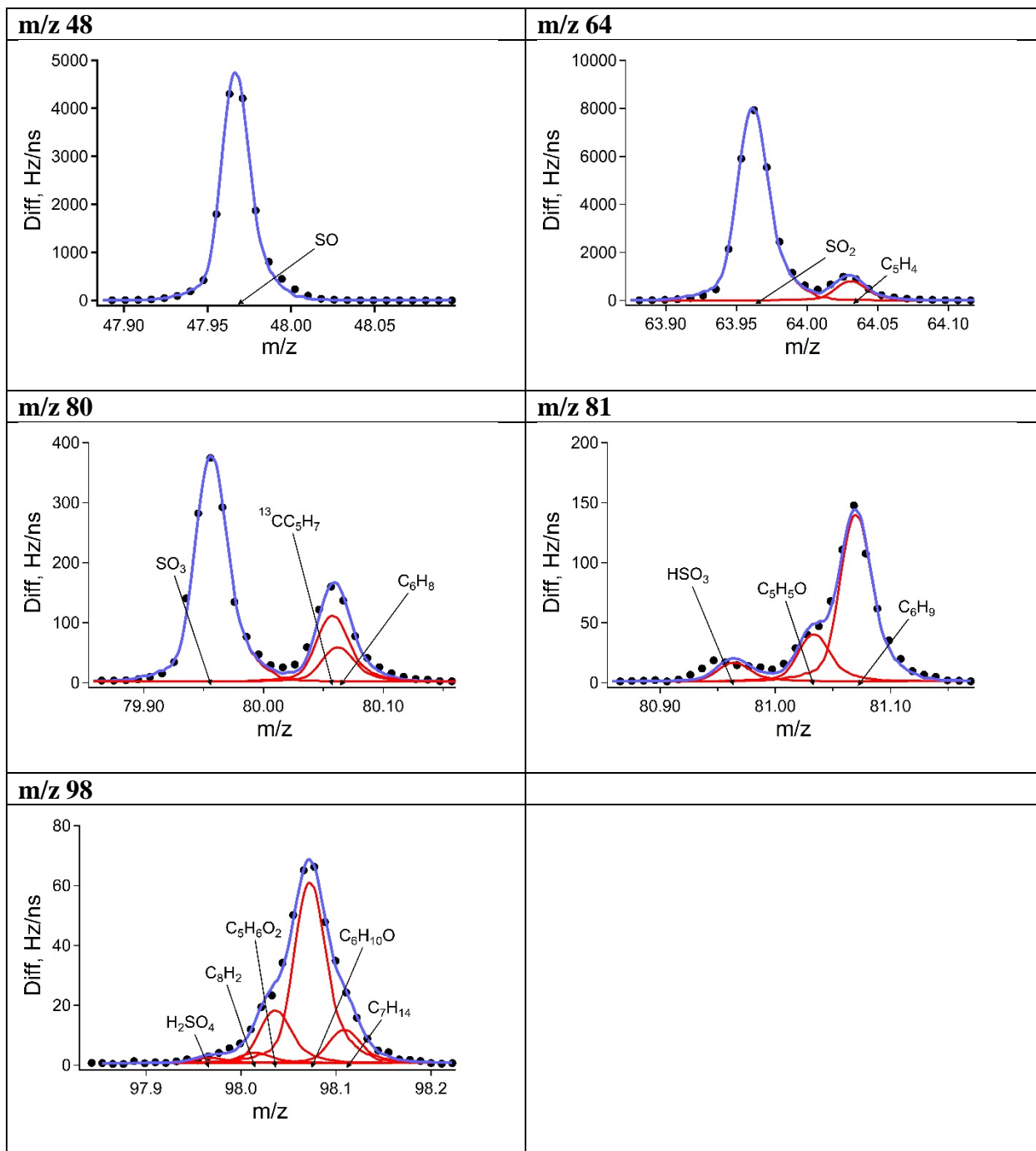
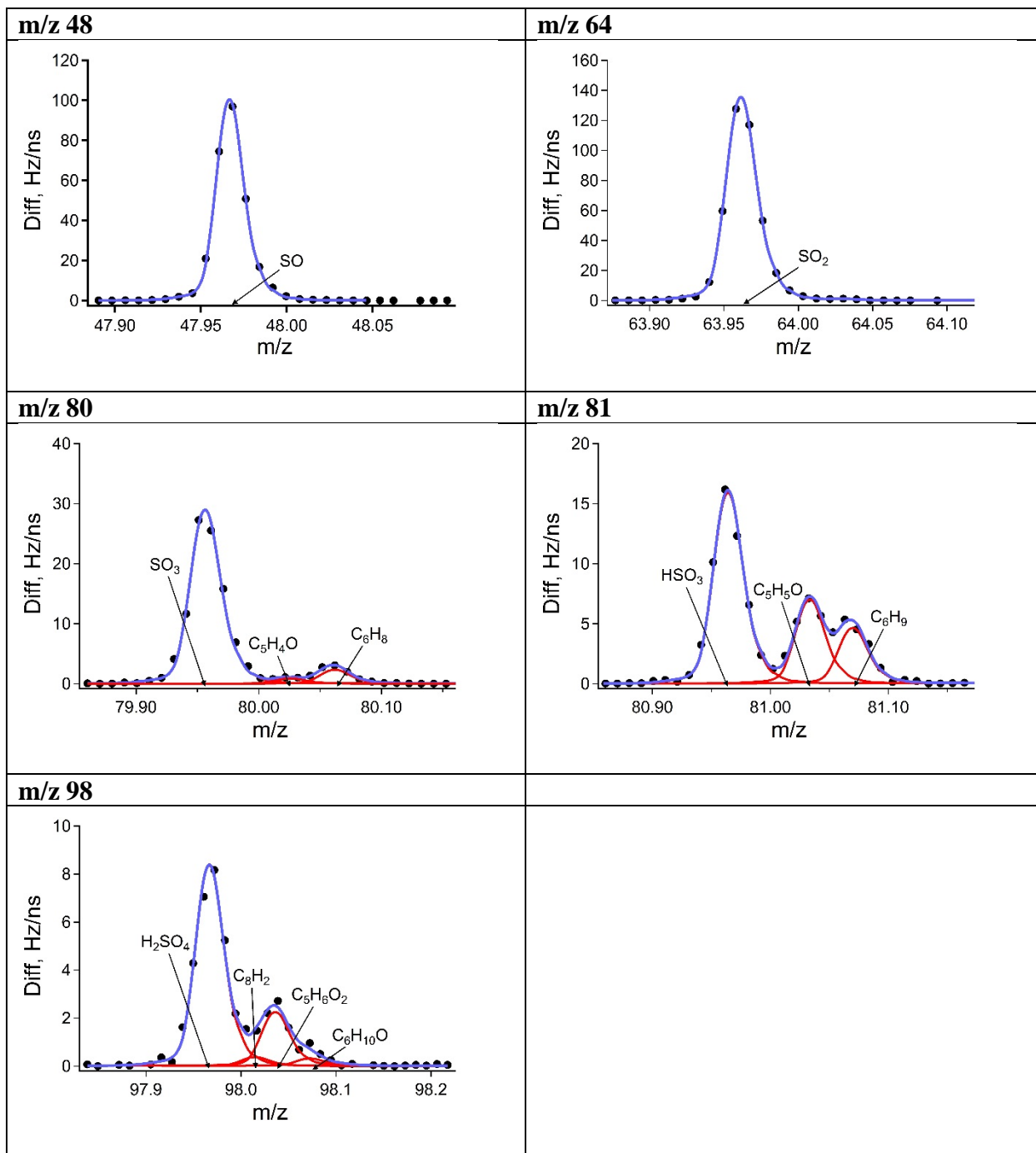**Figure S2** Peak fit of main sulfate fragments for OS-10.

117

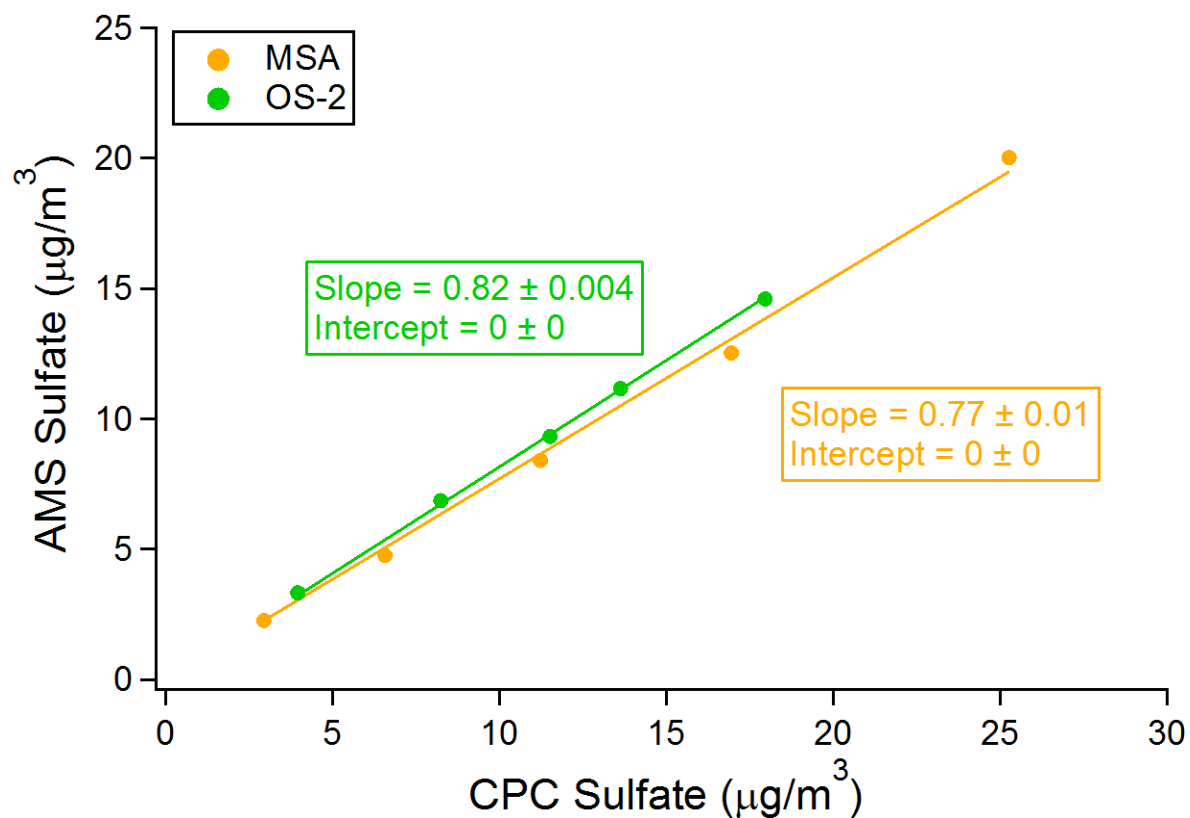**Figure S3** Peak fit of main sulfate fragments and CH$_3$SO$_2^+$ for MSA.

m/z 48

m/z 64

m/z 80

m/z 81

m/z 98

119

120 **Figure S4** Peak fit of main sulfate fragments for Centreville measurements.

Figure S5 RIE$_{SO4}$ calibration results for MSA and sodium ethyl sulfate (OS-2). The collection efficiency (CE) of 1 was applied to AMS data considering that atomized organosulfur particles were liquid droplets. The slope is acquired with intercept forced through zero.
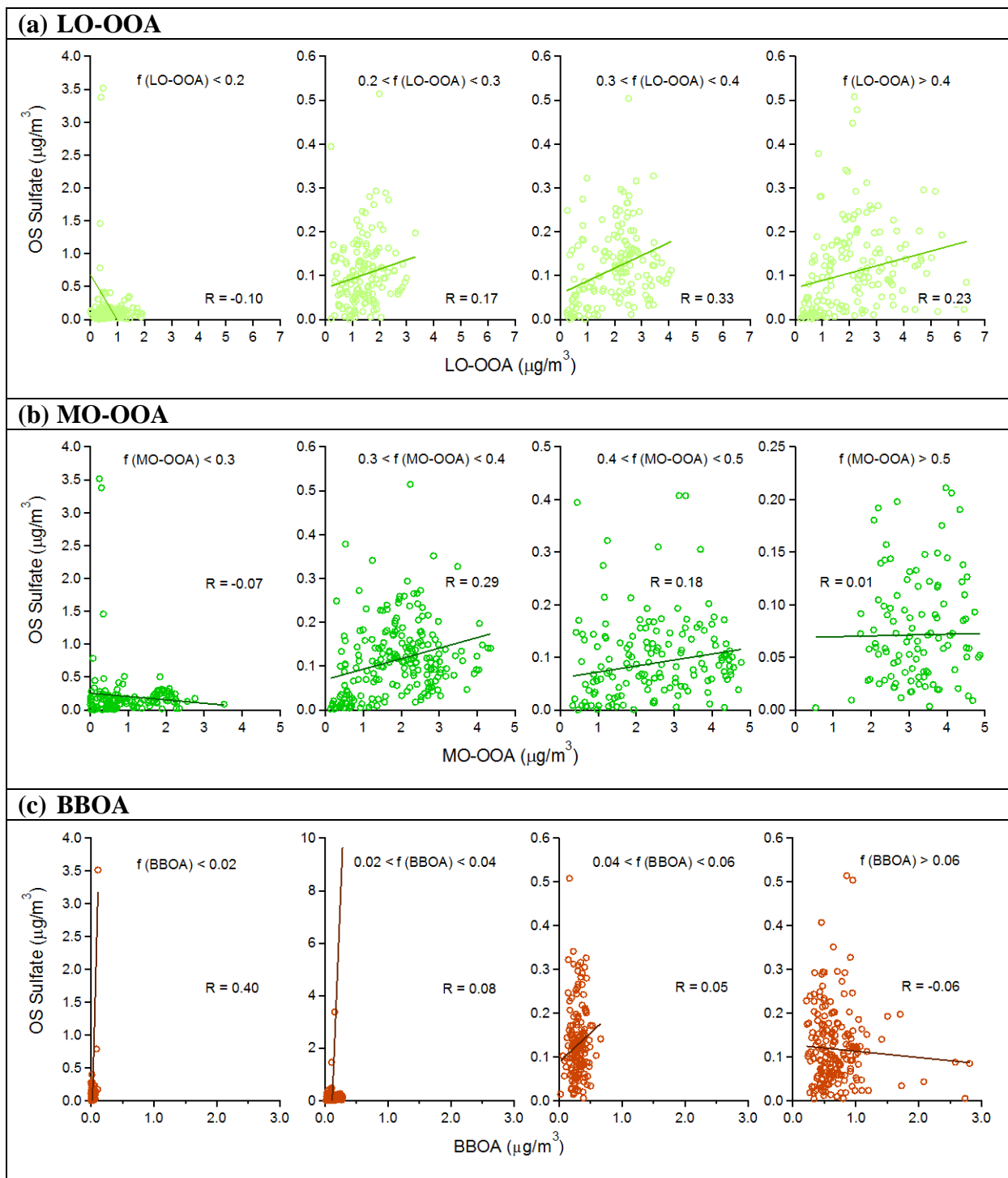
126

127
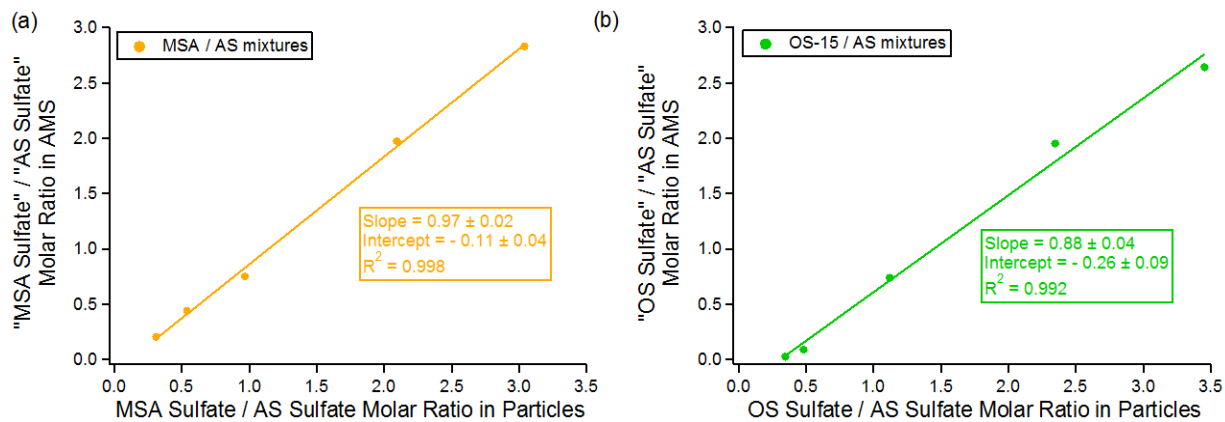
Figure S6 (a) "MSA sulfate" to "AS sulfate" ratio calculated by sulfate apportionment method as a function of MSA / AS molar ratio in particles. (b) "OS sulfate" to "AS sulfate" ratio calculated by sulfate apportionment method as a function of OS / AS molar ratio in particles for OS-15 / AS mixture. The slopes and intercepts are obtained by orthogonal distance regression (ODR). The Pearson's R is obtained by linear least-squares fit.
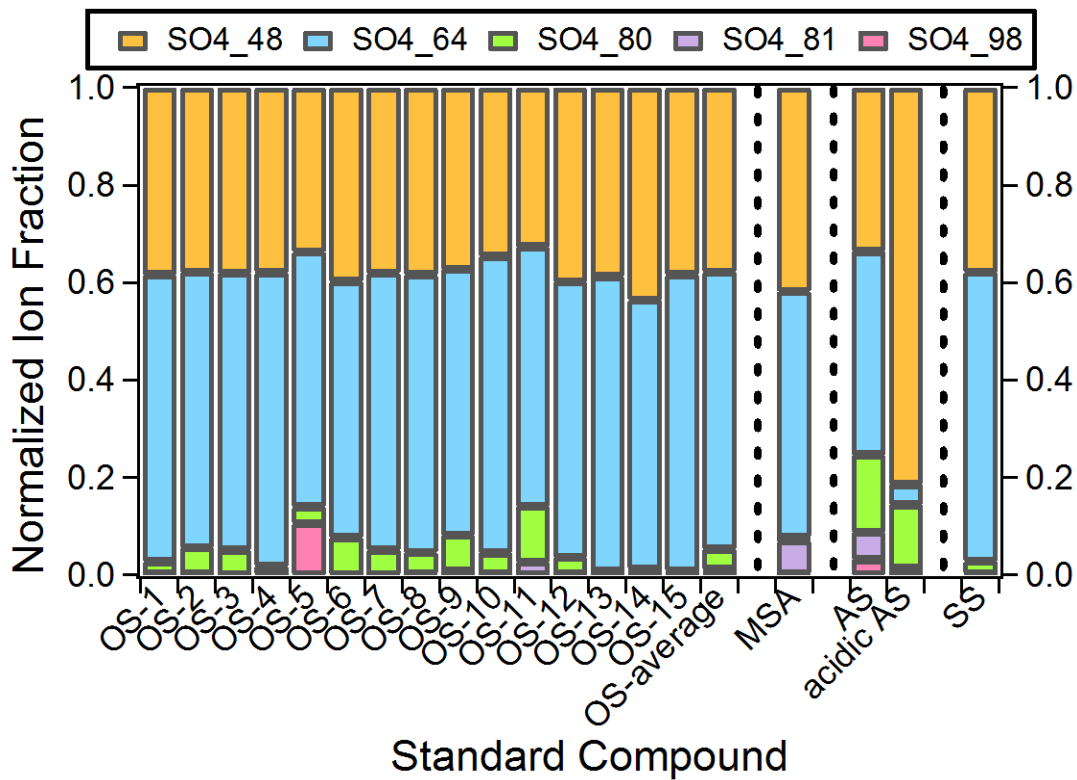
134

(a) Centreville

(b) Mace Head
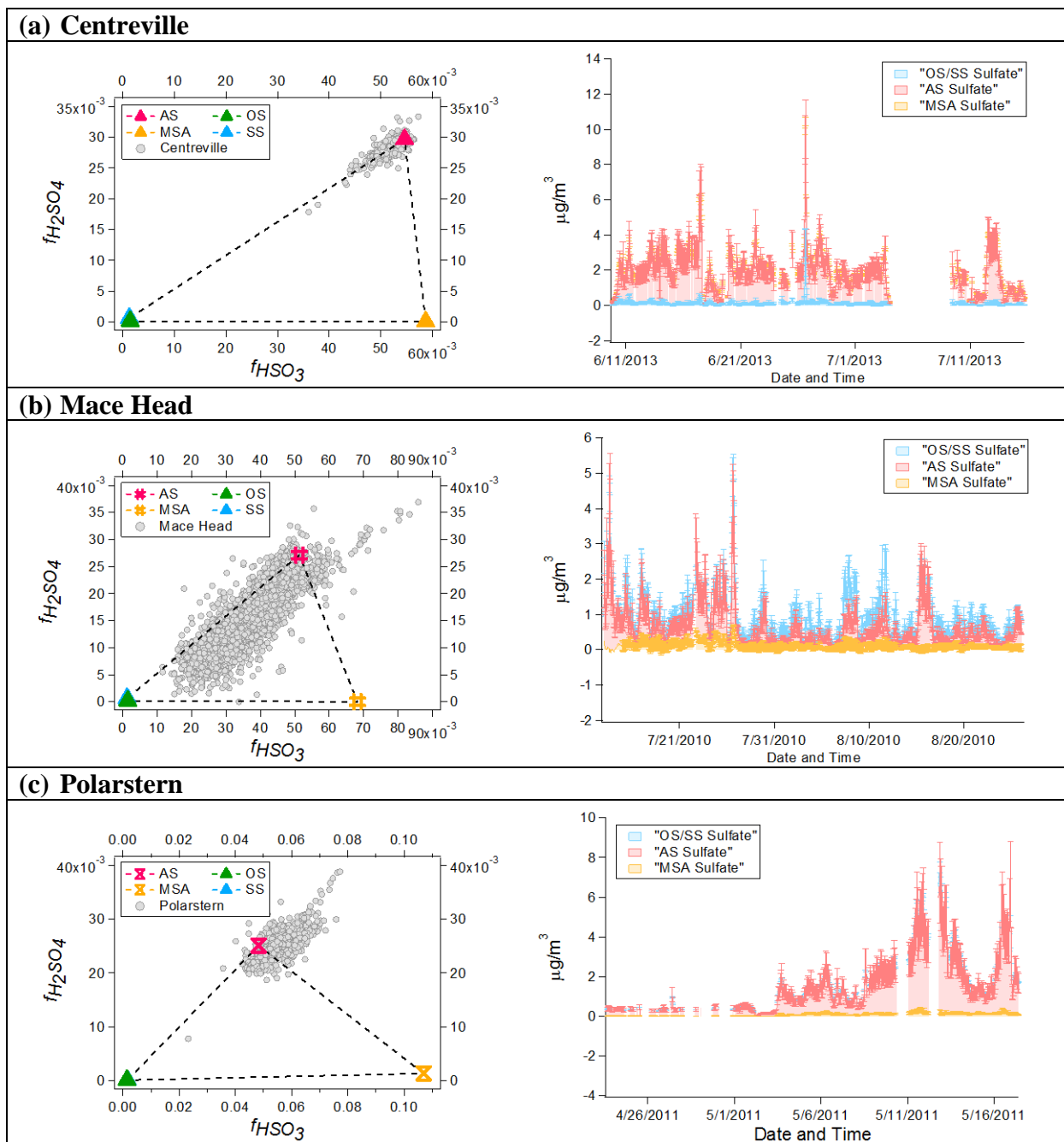
(c) Polarstern

Figure S7 $f_{H_2SO_4}$ vs. f_{HSO_3} for ambient measurements and time series of "AS sulfate", "OS/SS sulfate" and "MSA sulfate" for (a) Centreville; (b) Mace Head; (c) Polarstern. OS and SS standard calibrations are from GT AMS, while MSA and AS standard calibrations are from the AMS that was used for the corresponding ambient measurements.

Figure S8 Comparison of "OS sulfate" with (a) LO-OOA factor; (b) MO-OOA factor; (c) BBOA

factor for Centreville measurements. The AMS factor time series are from Xu et al. The Pearson's
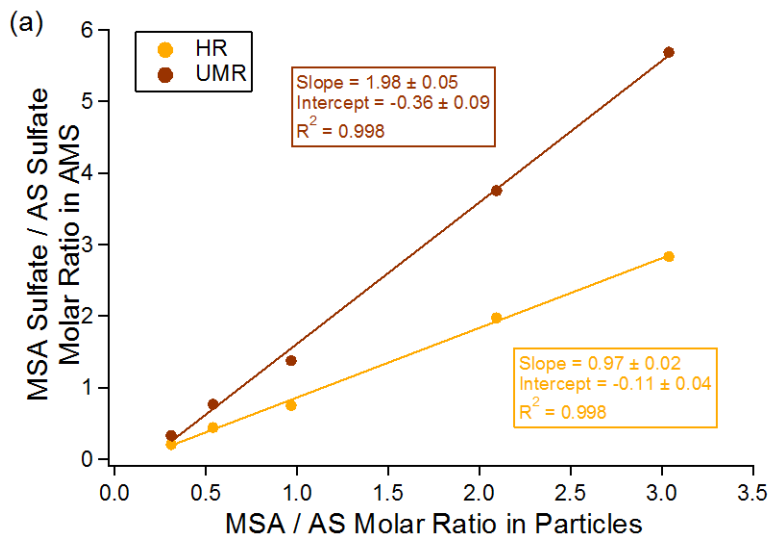
R is obtained by linear least-squares fit.
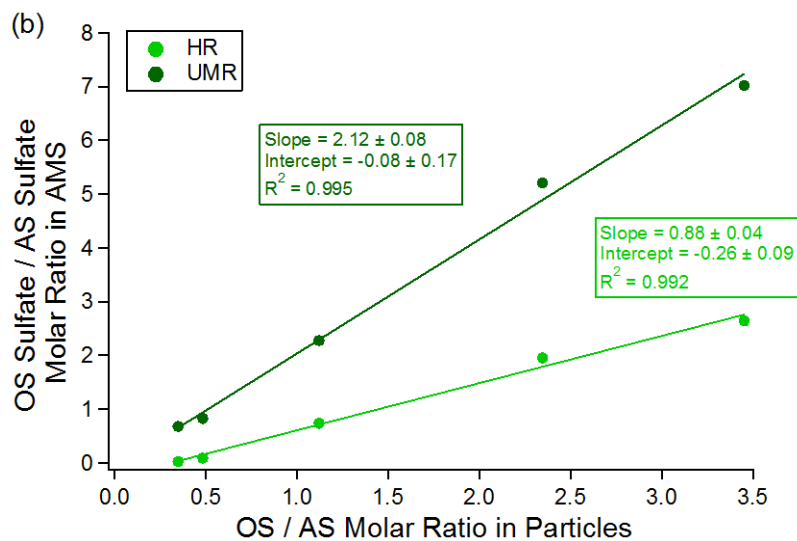
Figure S9 Mass fraction of five selected HSO ions.

(a)

Slope = 1.98 ± 0.05
Intercept = -0.36 ± 0.09
R^2 = 0.998

Slope = 0.97 ± 0.02
Intercept = -0.11 ± 0.04
R^2 = 0.998

MSA Sulfate / AS Sulfate Molar Ratio in AMS

MSA / AS Molar Ratio in Particles

148

149

(b)

Slope = 2.12 ± 0.08
Intercept = -0.08 ± 0.17
R^2 = 0.995

Slope = 0.88 ± 0.04
Intercept = -0.26 ± 0.09
R^2 = 0.992

OS Sulfate / AS Sulfate Molar Ratio in AMS

OS / AS Molar Ratio in Particles

150

Figure S10 HR and UMR comparisons of (a) "MSA sulfate" to "AS sulfate" ratio as a function of MSA / AS molar ratio in particles; (b) "OS sulfate" to "AS sulfate" ratio calculated by sulfate apportionment method as a function of OS / AS molar ratio in particles for OS-15 / AS mixture. The slopes and intercepts are obtained by orthogonal distance regression (ODR). The Pearson's R is obtained by linear least-squares fit.

156

157
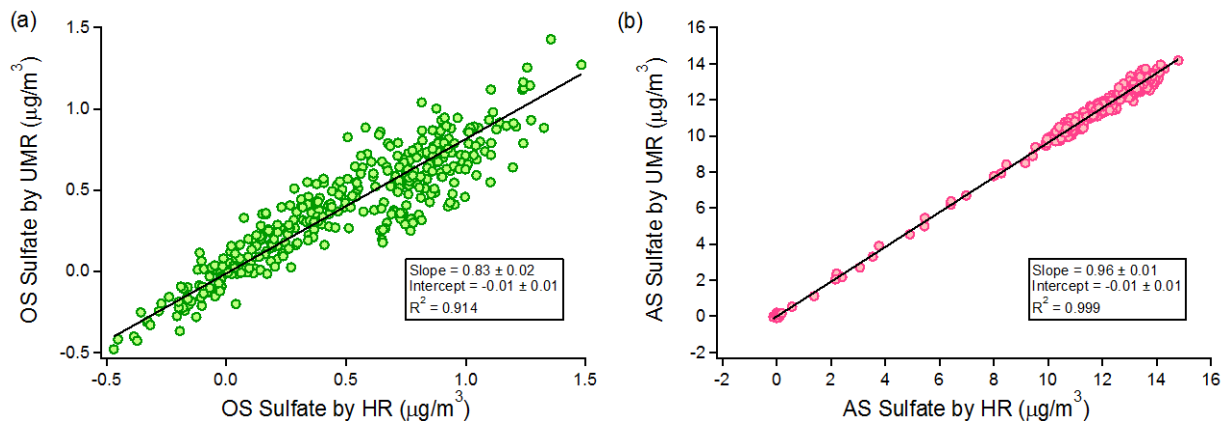
Figure S11 HR and UMR comparisons of (a) "OS sulfate" and (b) "AS sulfate" for the chamber isoprene photooxidation experiment. The slopes and intercepts are obtained by orthogonal distance regression (ODR). The Pearson's R is obtained by linear least-squares fit.
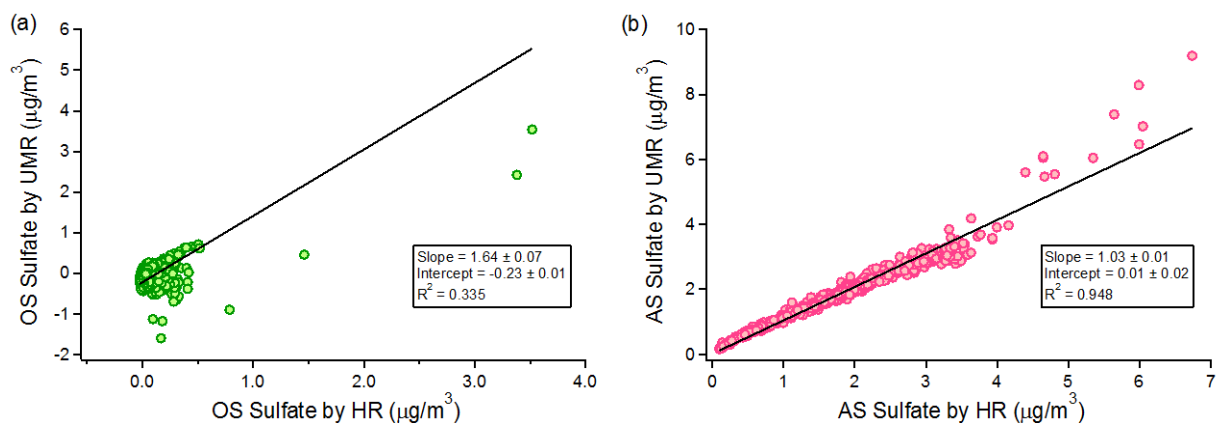
Figure S12 HR and UMR comparisons of (a) "OS sulfate" and (b) "AS sulfate" for Centreville measurements. The slopes and intercepts are obtained by orthogonal distance regression (ODR). The Pearson's R is obtained by linear least-squares fit.
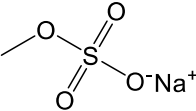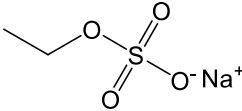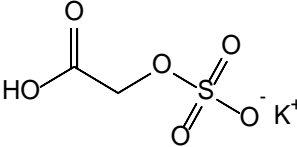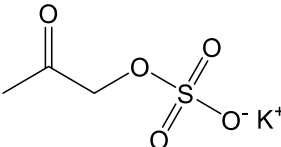
Table S1 *Table of Notations*
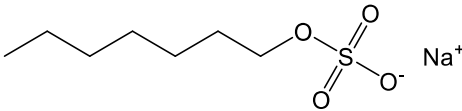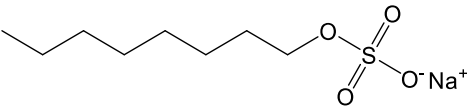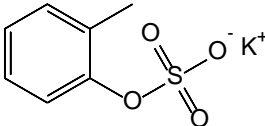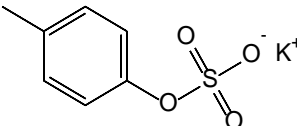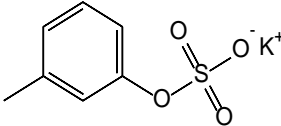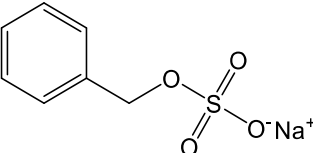
Notation	Description
AS	Ammonium sulfate
MSA	Methanesulfonic acid
OS	Organosulfur compounds except for MSA
SS	Sodium sulfate
Acidic AS	1:1 ammonium sulfate / sulfuric acid
Sulfate fragments	$H_xSO_y^+$ ions produced in AMS of both inorganic and organic origins
Organosulfur fragments	$C_xH_yO_zS^+$ ions produced in AMS by organosulfur compounds
ΣHSO	The sum of SO^+, SO_2^+, SO_3^+, HSO_3^+, and $H_2SO_4^+$ signals
$f_{H_2SO_4}$	The fraction of $H_2SO_4^+$ signal in ΣHSO
f_{HSO_3}	The fraction of HSO_3^+ signal in ΣHSO
"MSA Sulfate"	$H_xSO_y^+$ signals measured in AMS that attributed to MSA by sulfate apportionment method
"AS Sulfate"	$H_xSO_y^+$ signals measured in AMS that attributed to AS by sulfate apportionment method
"OS/SS Sulfate"	$H_xSO_y^+$ signals measured in AMS that attributed to OS/SS by sulfate apportionment method

169

170

171

Table S2 Standard Compounds

Compound	Molecular Structure	Family	Source
Sodium methyl sulfate (OS-1)		Organosulfate	Commercial (99%)
Sodium ethyl sulfate (OS-2)		Organosulfate	Commercial (96.31%)
Potassium glycolic acid sulfate (OS-3)		Organosulfate	Lab Synthesized[11] (> 98%)
Potassium hydroxyacetone sulfate (OS-4)		Organosulfate	Lab Synthesized[11] (> 98%)
Sodium n-heptyl sulfate (OS-5)		Organosulfate	Commercial (99%)
Sodium n-octyl sulfate (OS-6)		Organosulfate	Commercial (> 95%)
Potassium o-cresol sulfate (OS-7)		Organosulfate	Lab Synthesized[12] (> 98%)
Potassium p-cresol sulfate (OS-8)		Organosulfate	Lab Synthesized[12] (> 98%)
Potassium m-cresol sulfate (OS-9)		Organosulfate	Lab Synthesized[12] (> 98%)
Sodium benzyl sulfate (OS-10)		Organosulfate	Lab Synthesized[12] (> 98%)
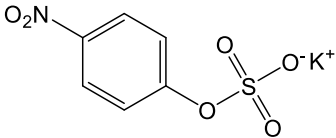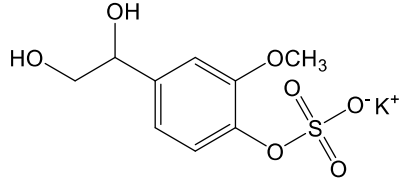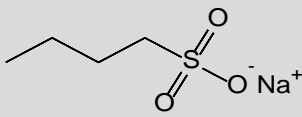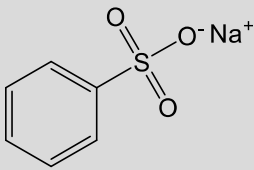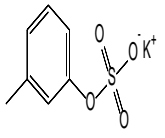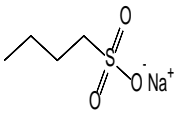
Potassium 4-nitrophenyl sulfate (OS-11)		Organosulfate	Commercial (> 98%)
Potassium 4-hydroxy-3-methoxyphenylglycol sulfate (OS-12)		Organosulfate	Commercial (> 98%)
Sodium 1-butanesulfonate (OS-13)		Sulfonate	Commercial (> 99%)
Sodium benzenesulfonate (OS-14)		Sulfonate	Commercial (97%)
Methanesulfonic acid (MSA)		Sulfonic Acid	Commercial (> 99%)
Ethanesulfonic acid (OS-15)		Sulfonic Acid	Commercial (95%)
Ammonium Sulfate (AS)	$(NH_4)_2SO_4$	Inorganic Sulfate	Commercial (> 99%)
Sodium Sulfate (SS)	Na_2SO_4	Inorganic Sulfate	Commercial (> 99%)

173

Table S3 Normalized Sulfate Fragments for Pure Compounds from GT AMS

Name	f_{SO}	f_{SO_2}	f_{SO_3}	f_{HSO_3}	$f_{H_2SO_4}$
OS-1	0.3760	0.6014	0.0215	0.0010	0.0000
OS-2	0.3821	0.5620	0.0528	0.0028	0.0003
OS-3	0.3686	0.6139	0.0174	0.0000	0.0002
OS-4	0.3755	0.6060	0.0184	0.0001	0.0000
OS-5	0.3655	0.5976	0.0364	0.0004	0.0000
OS-6	0.3864	0.5453	0.0671	0.0009	0.0002
OS-7	0.3772	0.5790	0.0433	0.0004	0.0001
OS-8	0.3735	0.5922	0.0336	0.0005	0.0002
OS-9	0.3754	0.5931	0.0310	0.0005	0.0000
OS-10	0.3664	0.6037	0.0285	0.0012	0.0002
OS-11	0.3684	0.5983	0.0333	0.0000	0.0000
OS-12	0.3807	0.5705	0.0481	0.0006	0.0001
OS-13	0.3754	0.6167	0.0061	0.0017	0.0001
OS-14	0.3712	0.6171	0.0044	0.0072	0.0001
OS-15	0.3796	0.6115	0.0021	0.0068	0.0000
MSA	0.4040	0.5358	0.0014	0.0587	0.0001
AS	0.3338	0.4223	0.1596	0.0546	0.0297
Acidic AS	0.3494	0.4667	0.0949	0.0567	0.0324
SS	0.3773	0.5914	0.0294	0.0013	0.0006

177

Table S4 Sulfate Fragmentation Table

Ion	HR_frag_sulfate (AS)	HR_frag_sulfate (MSA, OS, SS)
O	0.04*HR_frag_sulfate[{H2O}]	-
HO	0.25*HR_frag_sulfate[{H2O}]	-
j18O	0.00205499*HR_frag_sulfate[{O}]	-
H2O	0.67*HR_frag_sulfate[{SO2}], 0.67*HR_frag_sulfate[{SO}]	-
Hj18O	0.00205499*HR_frag_sulfate[{HO}]	-
H2j18O	0.00205499*HR_frag_sulfate[{H2O}]	-
S	0.21*HR_frag_sulphate[{SO2}], 0.21*HR_frag_sulphate[{SO}], 0.068*HR_frag_sulphate[{HSO3}], 0.068*HR_frag_sulphate[{H2SO4}]	0.21*HR_frag_sulphate[{SO2}], 0.21*HR_frag_sulphate[{SO}], 0.068*HR_frag_sulphate[{HSO3}], 0.068*HR_frag_sulphate[{H2SO4}]
j33S	0.00789557*HR_frag_sulphate[{S}]	0.00789557*HR_frag_sulphate[{S}]
j34S	0.0447416*HR_frag_sulphate[{S}]	0.0447416*HR_frag_sulphate[{S}]

178
179

180   **References**
181
182   1.   Boyd, C. M.; Sanchez, J.; Xu, L.; Eugene, A. J.; Nah, T.; Tuet, W. Y.; Guzman, M. I.;
183   Ng, N. L., Secondary organic aerosol formation from the β-pinene+NO$_3$ system:
184   effect of humidity and peroxy radical fate. *Atmos. Chem. Phys.* **2015,** *15*, (13), 7497-7522.
185   2.   Tuet, W. Y.; Chen, Y.; Xu, L.; Fok, S.; Gao, D.; Weber, R. J.; Ng, N. L., Chemical
186   oxidative potential of secondary organic aerosol (SOA) generated from the photooxidation of
187   biogenic and anthropogenic volatile organic compounds. *Atmos. Chem. Phys.* **2017,** *17*, (2), 839-
188   853.
189   3.   Xu, L.; Guo, H.; Boyd, C. M.; Klein, M.; Bougiatioti, A.; Cerully, K. M.; Hite, J. R.;
190   Isaacman-VanWertz, G.; Kreisberg, N. M.; Knote, C.; Olson, K.; Koss, A.; Goldstein, A. H.;
191   Hering, S. V.; de Gouw, J.; Baumann, K.; Lee, S. H.; Nenes, A.; Weber, R. J.; Ng, N. L., Effects
192   of anthropogenic emissions on aerosol formation from isoprene and monoterpenes in the
193   southeastern United States. *Proceedings of the National Academy of Sciences* **2015,** *112*, (1), 37-
194   42.
195   4.   Xu, L.; Suresh, S.; Guo, H.; Weber, R. J.; Ng, N. L., Aerosol characterization over the
196   southeastern United States using high-resolution aerosol mass spectrometry: spatial and seasonal
197   variation of aerosol composition and sources with a focus on organic nitrates. *Atmos. Chem.*
198   *Phys.* **2015,** *15*, (13), 7307-7336.
199   5.   Surratt, J. D.; Gómez-González, Y.; Chan, A. W. H.; Vermeylen, R.; Shahgholi, M.;
200   Kleindienst, T. E.; Edney, E. O.; Offenberg, J. H.; Lewandowski, M.; Jaoui, M.; Maenhaut, W.;
201   Claeys, M.; Flagan, R. C.; Seinfeld, J. H., Organosulfate Formation in Biogenic Secondary
202   Organic Aerosol. *The Journal of Physical Chemistry A* **2008,** *112*, (36), 8345-8378.
203   6.   Tolocka, M. P.; Turpin, B., Contribution of Organosulfur Compounds to Organic Aerosol
204   Mass. *Environmental Science & Technology* **2012,** *46*, (15), 7978-7983.
205   7.   Ovadnevaite, J.; Ceburnis, D.; Leinert, S.; Dall'Osto, M.; Canagaratna, M.; O'Doherty, S.;
206   Berresheim, H.; O'Dowd, C., Submicron NE Atlantic marine aerosol chemical composition and
207   abundance: Seasonal trends and air mass categorization. *Journal of Geophysical Research:*
208   *Atmospheres* **2014,** *119*, (20), 11,850-11,863.
209   8.   Huang, S.; Poulain, L.; van Pinxteren, D.; van Pinxteren, M.; Wu, Z.; Herrmann, H.;
210   Wiedensohler, A., Latitudinal and Seasonal Distribution of Particulate MSA over the Atlantic
211   using a Validated Quantification Method with HR-ToF-AMS. *Environmental Science &*
212   *Technology* **2017,** *51*, (1), 418-426.
213   9.   Schroder, J. C.; Campuzano-Jost, P.; Day, D. A.; Shah, V.; Larson, K.; Sommers, J. M.;
214   Sullivan, A. P.; Campos, T.; Reeves, J. M.; Hills, A.; Hornbrook, R. S.; Blake, N. J.; Scheuer, E.;
215   Guo, H.; Fibiger, D. L.; McDuffie, E. E.; Hayes, P. L.; Weber, R. J.; Dibb, J. E.; Apel, E. C.;
216   Jaeglé, L.; Brown, S. S.; Thornton, J. A.; Jimenez, J. L., Sources and Secondary Production of
217   Organic Aerosols in the Northeastern United States during WINTER. *Journal of Geophysical*
218   *Research: Atmospheres* **2018,** *123*, (14), 7771-7796.
219   10.   Bahreini, R.; Ervens, B.; Middlebrook, A. M.; Warneke, C.; de Gouw, J. A.; DeCarlo, P.
220   F.; Jimenez, J. L.; Brock, C. A.; Neuman, J. A.; Ryerson, T. B.; Stark, H.; Atlas, E.; Brioude, J.;
221   Fried, A.; Holloway, J. S.; Peischl, J.; Richter, D.; Walega, J.; Weibring, P.; Wollny, A. G.;
222   Fehsenfeld, F. C., Organic aerosol formation in urban and industrial plumes near Houston and
223   Dallas, Texas. *Journal of Geophysical Research: Atmospheres* **2009,** *114*, (D7).

224 11.   Hettiyadura, A. P. S.; Stone, E. A.; Kundu, S.; Baker, Z.; Geddes, E.; Richards, K.;
225 Humphry, T., Determination of atmospheric organosulfates using HILIC chromatography with
226 MS detection. *Atmos. Meas. Tech.* **2015,** *8*, (6), 2347-2358.
227 12.   Staudt, S.; Kundu, S.; Lehmler, H.-J.; He, X.; Cui, T.; Lin, Y.-H.; Kristensen, K.;
228 Glasius, M.; Zhang, X.; Weber, R. J.; Surratt, J. D.; Stone, E. A., Aromatic organosulfates in
229 atmospheric aerosols: Synthesis, characterization, and abundance. *Atmospheric Environment*
230 **2014,** *94*, 366-373.

231